Report

Current Biology

Earliest Mysticete from the Late Eocene of Peru Sheds New Light on the Origin of Baleen Whales

Highlights

- An ancient whale is described based on a skeleton from the late Eocene of Peru
- It is identified as the earliest known mysticete (baleen whales and relatives)
- Skeletal anatomy provides crucial information on archaeocete-mysticete transition
- This whale is interpreted as specialized for suction and possibly benthic feeding

Authors

Olivier Lambert, Manuel Martínez-Cáceres, Giovanni Bianucci, ..., Etienne Steurbaut, Mario Urbina, Christian de Muizon

Correspondence

olivier.lambert@naturalsciences.be

In Brief

Lambert et al. describe a new toothed cetacean from the late Eocene of Peru. Being the oldest known baleen whale relative (Mysticeti), its skeletal morphology provides crucial information about the archaeocete-neocete transition, suggesting a specialization toward suction and possibly benthic feeding early in the mysticete evolutionary history.

Lambert et al., 2017, Current Biology *27*, 1535–1541
May 22, 2017
http://dx.doi.org/10.1016/j.cub.2017.04.026

CellPress

Current Biology
Report

Earliest Mysticete from the Late Eocene of Peru Sheds New Light on the Origin of Baleen Whales

Olivier Lambert,[1,7,*] Manuel Martínez-Cáceres,[2] Giovanni Bianucci,[3] Claudio Di Celma,[4] Rodolfo Salas-Gismondi,[5] Etienne Steurbaut,[1,6] Mario Urbina,[5] and Christian de Muizon[2]
[1]D.O. Terre et Histoire de la Vie, Institut Royal des Sciences Naturelles de Belgique, Rue Vautier 29, 1000 Brussels, Belgium
[2]Centre de Recherche sur la Paléobiodiversité et les Paléoenvironnements-CR2P (CNRS, MNHN, UPMC, Sorbonne Université), Département Origines et Évolution, Muséum National d'Histoire Naturelle, Rue Buffon 8, 75005 Paris, France
[3]Dipartimento di Scienze della Terra, Università di Pisa, Via S. Maria 53, 56126 Pisa, Italy
[4]Scuola di Scienze e Tecnologie, Università di Camerino, Via Gentile III da Varano 1, 62032 Camerino, Italy
[5]Departamento de Paleontología de Vertebrados, Museo de Historia Natural-UNMSM, Avenida Arenales 1256, 14 Lima, Peru
[6]Department of Earth and Environmental Sciences, KU Leuven, Celestijnenlaan 200E, 3001 Leuven, Belgium
[7]Lead Contact
*Correspondence: olivier.lambert@naturalsciences.be
http://dx.doi.org/10.1016/j.cub.2017.04.026

SUMMARY

Although combined molecular and morphological analyses point to a late middle Eocene (38–39 million years ago) origin for the clade Neoceti (Odontoceti, echolocating toothed whales plus Mysticeti, baleen whales, and relatives), the oldest known mysticete fossil dates from the latest Eocene (about 34 million years ago) of Antarctica [1, 2]. Considering that the latter is not the most stemward mysticete in recent phylogenies and that Oligocene toothed mysticetes display a broad morphological disparity most likely corresponding to contrasted ecological niches, the origin of mysticetes from a basilosaurid ancestor and its drivers are currently poorly understood [1, 3–8]. Based on an articulated cetacean skeleton from the early late Eocene (Priabonian, around 36.4 million years ago) of the Pisco Basin, Peru, we describe a new archaic tooth-bearing mysticete, *Mystacodon selenensis* gen. et sp. nov. Being the geologically oldest neocete (crown group cetacean) and the earliest mysticete to branch off described so far, the new taxon is interpreted as morphologically intermediate between basilosaurids and later toothed mysticetes, providing thus crucial information about the anatomy of the skull, forelimb, and innominate at these critical initial stages of mysticete evolution. Major changes in the morphology of the oral apparatus (including tooth wear) and flipper compared to basilosaurids suggest that suction and possibly benthic feeding represented key, early ecological traits accompanying the emergence of modern filter-feeding baleen whales' ancestors.

RESULTS

Systematics

Cetacea
Pelagiceti
Neoceti
Mysticeti
Mystacodontidae fam. nov.
Mystacodon selenensis gen. et sp. nov.

Etymology

From ancient Greek *mystacos* ("moustache") in reference to the suborder Mysticeti and *odontos* ("tooth"), "mysticete with teeth," and from *Selene*, the Greek goddess of the moon, in reference to the Playa Media Luna type locality.

Holotype

Museo de Historia Natural, Universidad Nacional Mayor de San Marcos (MUSM; Lima, Peru) 1917, partial skeleton including cranium, mandibles, teeth, cervical, thoracic, lumbar and caudal vertebrae, ribs, partial right and left forelimbs, and left innominate.

Locality

Playa Media Luna, southern part of Pisco Basin, southern coast of Peru, 14° 36′ 07.5″ S, 75° 54′ 48.3″ W (Figures S1B–S1D).

Horizon

Middle part of the Yumaque Formation, 77 m above the base; lower part of calcareous nannofossil zone NP19/20 of Martini [9]; dated at 36.4 million years ago based on age estimations used by Agnini et al. [10]; early late Eocene (early Priabonian; see Figures S1A and S1D, Table S1, and STAR Methods for the biostratigraphic and biochronological interpretations).

Diagnosis

MUSM 1917 is identified as a Neoceti based on the following derived characters, absent in basilosaurid archaeocetes: partly open mesorostral groove; anteroposteriorly elongated rostral portion of maxilla; loss of sagittal crest; supraoccipital shield anterodorsally inclined; apex of zygomatic process of squamosal nearly contacting postorbital process of frontal; and distal epiphysis of the humerus divided in two angled radial and ulnar facets. It can be referred to the Mysticeti due to the following combination of derived characters: dorsoventrally thin lateral edge of maxilla on rostrum; presence of an antorbital process of the

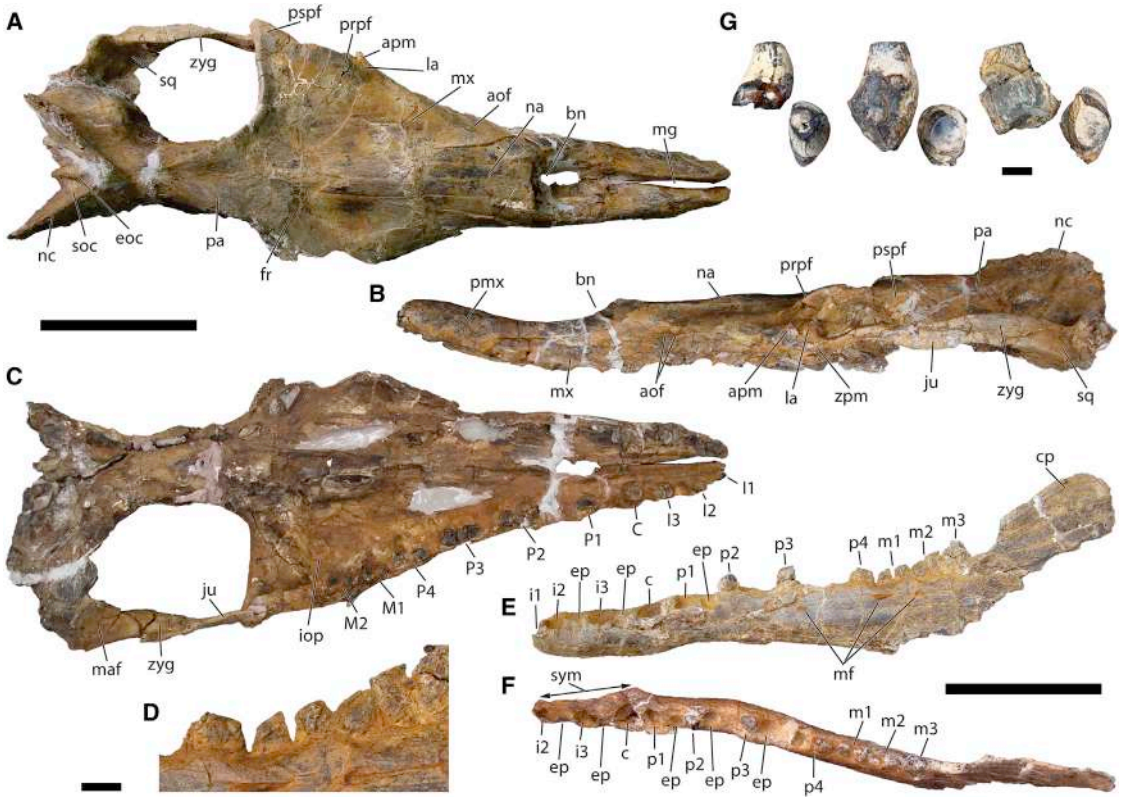

Figure 1. Cranium, Mandible, and Teeth of *Mystacodon selenensis* gen. et sp. nov. MUSM 1917

Cranium in dorsal (A), left lateral (B), and ventral (C) views; detail of left posterior lower teeth in lateral view (D); left mandible in lateral (E) and dorsal (F) views; and three detached anterior lower teeth (from left to right: incisor, incisor/canine, and ?p1) in lingual or labial and occlusal views (G). aof, antorbital foramina; apm, antorbital process of maxilla; bn, bony nares; C, upper canine; c, lower canine; cp, coronoid process; ep, embrasure pit; I1–I3, upper incisors; i1–i3, lower incisors; iop, infraorbital plate; ju, jugal; la, lacrimal; M1 and M2, upper molars; m1–m3, lower molars; maf, mandibular fossa; mf, mental foramina; mg, mesorostral groove; mx, maxilla; na, nasal; nc, nuchal crest; P1–P4, upper premolars; p1–p4, lower premolars; pa, parietal; pmx, premaxilla; prpf, preorbital process of frontal; pspf, postorbital process of frontal; sq, squamosal; sym, mandibular symphysis; zpm, zygomatic process of maxilla; zyg, zygomatic process of squamosal. Scale bars for (A)–(C), (E), and (F), 200 mm; for (D), 20 mm; and for (G), 10 mm. See also Figures S2 and S4 and Table S2.

maxilla; presence of a maxillary infraorbital plate; and triangular supraoccipital shield. It is further diagnosed by two possibly autapomorphic features: nasal anteroposteriorly longer than frontal plus parietal and strong tuberosity on anterior edge of radius; two additional derived characters: posteriormost upper tooth anterior to level of antorbital process of maxilla and broad-based rostrum (ratio between width of skull at rostrum base and width at postorbital process > 0.8); and a series of plesiomophic features: supraoccipital shield not extending anterior to anterior level of squamosal fossa, only two dorsal infraorbital foramina, a basilosaurid dental formula 3.1.4.2/3.1.4.3, no wide diastemata between posterior cheek teeth, sutured mandibular symphysis, and well-defined acetabulum on innominate. Finally, MUSM 1917 lacks cranial synapomorphies of Odontoceti: facial concavity, presence of premaxillary foramen and premaxillary sac fossa, and posterior expansion of maxilla over the supraorbital region (see [1, 5, 11–13]) (Figures 1, 2, 3, and S2).

Phylogenetic Analysis

To test the phylogenetic affinities of *Mystacodon selenensis*, we modified the matrix of a previous analysis [1] (see STAR Methods). The consensus tree obtained (from two trees) with the heuristic search resulted in a topology very similar to that of Marx and Fordyce [1], with a monophyletic Mysticeti. In this tree (Figure 4), *M. selenensis* is the first mysticete to branch off, followed by a clade including Aetiocetidae and Mammalodontidae, ChM PV4745 (an unnamed Oligocene toothed mysticete from North Carolina), and *Llanocetus denticrenatus*, the latter being a sister group to baleen-bearing mysticetes (Chaeomysticeti).

Size Estimates

With the condylobasal length of the cranium close to 1 m and a bizygomatic width of 40 cm (Table S2), *Mystacodon selenensis* was a small to medium size mysticete, considerably smaller than the latest Eocene *Llanocetus denticrenatus*, but larger than nearly all Oligocene toothed mysticetes [5, 15] (Figure 4). Its total body length was estimated based on equations provided by Lambert et al. [16] and Pyenson and Sponberg [17] (see STAR Methods); it probably ranged between 3.75 m and 4 m.

Brief Description and Comparison

In addition to the characters mentioned in the diagnosis, the cranium of *M. selenensis* is strongly dorsoventrally flattened

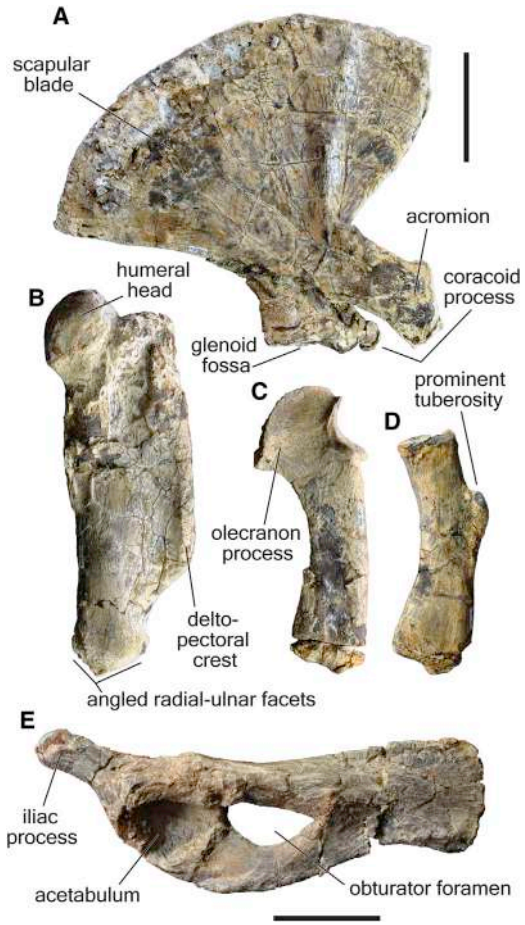

Figure 2. Postcranial Elements of *Mystacodon selenensis* gen. et sp. nov. MUSM 1917

Right scapula (A), humerus (B), ulna (C), and radius (D) in lateral view and left innominate (E) in lateral view. Scale bars for (A)–(D), 100 mm; for (E), 50 mm. See also Figure S4.

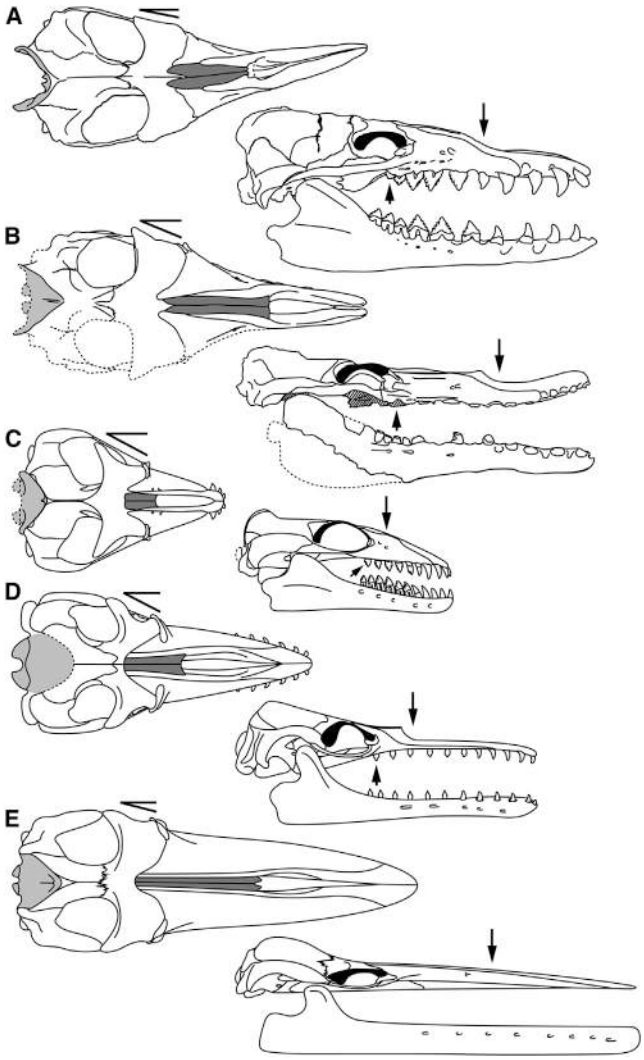

Figure 3. Comparison of the Skull of *Mystacodon selenensis* gen. et sp. nov. with a Basilosaurid Archaeocete and Several Early Mysticetes

Schematic dorsal and right lateral views for the cranium and mandible of the basilosaurid *Cynthiacetus peruvianus* (A), the tooth-bearing mysticetes *Mystacodon selenensis* gen. et sp. nov. (lateral views reversed from left side; B), *Janjucetus hunderi* (C), and *Aetiocetus weltoni* (D) and the edentulous eomysticetid *Yamatocetus canaliculatus* (E). Black areas, lateralmost part of orbit; medium gray, nasals; and light gray, occipital shield. Upper arrows indicate the level of the bony nares; lower arrows indicate the level of the last cheek tooth. The angle between the lateral margin of the orbit and the longitudinal axis is illustrated with two thick black lines in dorsal view. All crania reduced to the same bizygomatic width. (A) was modified from [11], and (C)–(E) were modified from [8]. See also Figure S3.

when compared to basilosaurids (Figure 1B). Still, it retains a concave lateral margin of the rostrum in dorsal view (Figure 1A). The bony nares are transversely wide, and the postnarial length of the rostrum is considerably longer than in basilosaurids (Figures 1 and 3), representing 63% of the bizygomatic width. The dorsal infraorbital foramina are far anterior to the antorbital process of the maxilla, at the anterior end of a wide, dorsolaterally facing surface of the maxilla. The orbit of *M. selenensis* is proportionally larger, more anteriorly oriented, with a slightly concave lateral edge, and more elevated relatively to the skull roof than in basilosaurids and extant mysticetes, thus resembling several other tooth-bearing mysticetes (Figures 3 and S3). The intertemporal region is short and transversely broad, laterally defined by developed orbitotemporal crests. The short supraoccipital shield is transversely wider than that in basilosaurids; it bears a prominent external occipital crest and is markedly pointed anterodorsally. The elongated zygomatic process of the squamosal displays a dorsoventrally low distal portion and an extended contact with the styliform process of the jugal (Figures 1 and S2C). Whereas deep embrasure pits are observed between anterior upper teeth, only short diastemata separate posterior cheek teeth (Figures 1, S2C, S2D, and S2F).

Contrasting with other toothed mysticetes, the dentary is laterally concave in the dorsal view (Figures 1F and S2F). Extending until the level of the canine, the mandibular symphysis is shorter than in basilosaurids but is markedly longer than in other mysticetes [11, 13, 18].

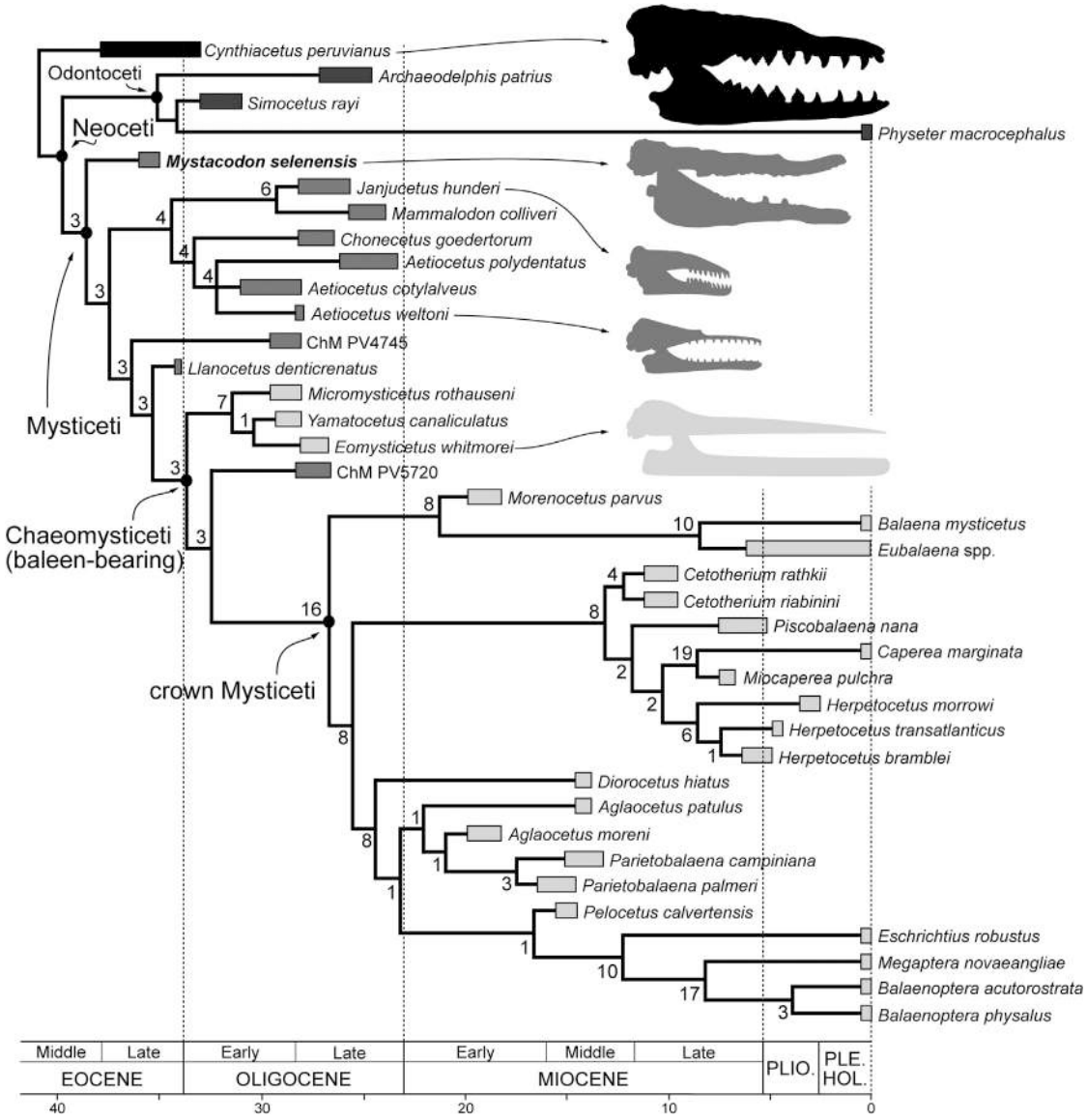

Figure 4. Phylogenetic Relationships of *Mystacodon selenensis*

Strict consensus tree of two most parsimonious trees resulting from analysis of 272 characters and 38 taxa, focusing on the relationships within stem Mysticeti. *M. selenensis* is in bold. Numbers associated with ingroup nodes are Bremer support values. Thick bars indicate temporal ranges of taxa. Black filling, Basilosauridae; dark gray, Odontoceti; medium gray, toothed Mysticeti; and light gray, Chaeomysticeti (baleen-bearing Mysticeti). All silhouettes of skulls are at the same scale. The character-taxon matrix was modified from [1]. Data for temporal ranges were taken from [1, 11, 14].

Posterior premolars and molars are double rooted. All of the preserved teeth are apically truncated, with a flat wear surface (Figures 1B, 1D, 1G, and 1E). Taking into account the observed embrasure pits in the upper and lower jaws, the truncated apices are interpreted as resulting from abrasion (versus attrition). The similar degree of wear in different posterior lower teeth may indicate that wear occurred locally roughly until the level of a relatively high gum (e.g., [19]).

On the well-preserved forelimb, the humerus is roughly as long as the scapula but is considerably longer than the radius and ulna (Figures 2A–2D), a condition shared, among others, with several slow-swimming extant cetaceans [20]. As in nearly all other neocetes (see [12] for an exception), considering the distinctly angled radial and ulnar facets, the elbow articulation was ankylosed. The acromion of the scapula is anteroventrally projected, and the anterior edge of the radius bears a prominent tuberosity, which is not observed in any other cetacean.

The anterior portion of the innominate of *Mystacodon selenensis* is strikingly basilosaurid like in outline, with a short and massive iliac process and a well-defined acetabulum (Figure 2E). The obturator foramen is proportionally large and the portion of bone posterior to the foramen is shortened compared to the basilosaurids *Basilosaurus* and *Chrysocetus*.

DISCUSSION

Compared to basilosaurids, the shortening of the prenarial part of the rostrum and the shorter mandibular symphysis in *Mystacodon selenensis* point to a reduced use of the incisor-bearing, grasping part of the snout, whereas the broader and proportionally longer postnarial region indicates a greater volume for the posterior part of the oral cavity. Furthermore, the presence of a maxillary infraorbital plate allows for the oral cavity to be separated from the orbit region by a rigid element, and closely applied posterior cheek teeth further contribute to the lateral closure of this larger cavity. All together, these changes in the configuration of the oral apparatus suggest a higher degree of specialization for suction-assisted feeding in *M. selenensis* [18, 21, 22], contrasting with the raptorial feeding strategies proposed for basilosaurids [23, 24]. This hypothesis is further supported by the loss of the sagittal crest and the markedly reduced height of the neurocranium in *M. selenensis*, corresponding to a reduction of the surfaces of origin of the temporal muscles. On the other side, although the preservation state of the palate of the holotype does not allow for assessment of the presence or absence of palatal sulci and thus the hypothetical presence or absence of proto-baleen [4], *M. selenensis* unambiguously lacks the main skull features associated with bulk filter feeding in baleen-bearing mysticetes: edentulous jaws, laterally bowed mandibles, non-sutured mandibular symphysis, and cranial kinesis [18, 19, 25]. Interestingly, suction feeding has been recently proposed as a key transitional feeding technique between raptorial feeding in basilosaurid ancestors and filter feeding in other, more crownward toothed mysticetes ([18, 19, 26]; but see also an alternative scenario in [4, 27]). This interpretation lends support to our observations, which suggest that *M. selenensis* already acquired some degree of suction feeding ability.

Resulting from the contact with either abrasive food items or abrasive particles accidentally ingested during prey capture along the seafloor (a hypothesis further supported by the position, orientation, and size of orbits [5]), the planar dental wear pattern in *Mystacodon selenensis* is strongly reminiscent of the apical wear observed in the short-snouted toothed mysticete *Mammalodon* and several odontocetes [5, 28, 29] and departs markedly from the wear patterns in basilosaurids [11, 13].

From a locomotion viewpoint, the combination of the immobile elbow with the anteroventrally projected acromion of the scapula and the prominent tuberosity on the anterior edge of the radius suggest a unique condition for the muscles extending the flipper (m. brachialis and deltoideus), differing from both basilosaurids and other known neocetes [13, 30]. Due to the lack of a modern equivalent, the functional bearings of such a condition on the use of the flipper are not fully understood, but this denotes a major change from the basilosaurid condition, possibly related to benthic feeding (assistance of the forelimb for moving along the seafloor or for maintaining a static position; Figure S4). Unfortunately, the forelimb is currently unknown in other presumably benthic feeding toothed mysticetes [5].

Taking into account the evolutionary scenario recently proposed for more crownward toothed mysticetes [19], we conclude that the observed tooth wear and the skull and forelimb morphology of *M. selenensis* testify for a main ecological shift at the basilosaurid-mysticete transition and that adaptation to suction on individual, small-size prey and possibly benthic feeding resulted in the emergence of the earliest toothed mysticetes.

The basilosaurid-like condition of the innominate in *Mystacodon selenensis* indicates that the articulated hind limb of this new mysticete was probably still protruding from the abdominal wall (Figure S4). Such a condition in an early mysticete suggests that the last steps of the evolutionary reduction of the hind limb did not occur in the last common ancestor of odontocetes and mysticetes as previously thought [31], but later, independently in the two modern lineages.

As a perspective for future work, it is worth noting that, contrasting with ancient mysticetes (including *Mystacodon selenensis*), from a morphological viewpoint, the earliest odontocetes depart markedly from a hypothetical basilosaurid ancestor. Indeed, the oldest extinct odontocetes being described are dated from the Oligocene [12, 32, 33], and the early evolutionary history of echolocating toothed whales is thus poorly constrained. The study of older, earliest Oligocene [34] and even late Eocene forms will be crucial for elucidating the first steps of the evolution of this other, highly successful cetacean lineage.

STAR★METHODS

Detailed methods are provided in the online version of this paper and include the following:

- KEY RESOURCES TABLE
- CONTACT FOR REAGENT AND RESOURCE SHARING
- METHOD DETAILS
  - Geological Context and Biostratigraphy
  - Phylogenetic Analysis
- QUANTIFICATION AND STATISTICAL ANALYSIS
- DATA AND SOFTWARE AVAILABILITY

SUPPLEMENTAL INFORMATION

Supplemental Information includes four figures, two tables, and one data file and can be found with this article online at http://dx.doi.org/10.1016/j.cub.2017.04.026.

AUTHOR CONTRIBUTIONS

M.U. discovered the specimen MUSM 1917; C.d.M., G.B., M.M.-C., M.U., O.L., and R.S.-G. took part in the excavation of the skeleton; C.D.C. analyzed the geological context and elaborated the stratigraphical section; E.S. undertook the biostratigraphical analyses; C.d.M. performed the phylogenetic analysis with input from G.B. and O.L.; C.D.C., C.d.M., G.B., M.M.-C., and O.L. prepared the figures; and O.L. wrote the manuscript with input from all authors.

ACKNOWLEDGMENTS

We thank W. Aguirre, E. Díaz, and R. Varas-Malca for their help during fieldwork in November 2010, W. Aguirre for the careful preparation of MUSM 1917, R. Varas-Malca for giving access to the MUSM collection, K. Gariboldi for her advice on Paleogene diatom zonations, E. Malinverno for her help during the preparation of the geological section at Playa Media Luna and for kindly providing a series of sediment samples for biostratigraphical analyses, R.E. Fordyce and F.G. Marx for sending us photos of the holotype of *Llanocetus denticrenatus*, A. Gennari for preparing the life reconstruction of *Mystacodon selenensis*, and R.A. Racicot and an anonymous reviewer for their constructive comments. Field expedition during which the skeleton MUSM 1970 has been collected was funded by the Muséum National d'Histoire Naturelle, Paris (Action Transversale "Biodiversité Actuelle et Fossile" 2010).

Geological and stratigraphical field investigations were supported by a grant of the Italian Ministero dell'Istruzione dell'Università e della Ricerca (PRIN Project 2012YSBMK).

Received: March 14, 2017
Revised: April 4, 2017
Accepted: April 13, 2017
Published: May 11, 2017

REFERENCES

1. Marx, F.G., and Fordyce, R.E. (2015). Baleen boom and bust: a synthesis of mysticete phylogeny, diversity and disparity. R. Soc. Open Sci. *2*, 140434.
2. Mitchell, E.D. (1989). A new cetacean from the Late Eocene La Meseta Formation Seymour Island, Antarctic Peninsula. Can. J. Fish. Aquat. Sci. *46*, 2219–2235.
3. Fitzgerald, E.M.G. (2006). A bizarre new toothed mysticete (Cetacea) from Australia and the early evolution of baleen whales. Proc. Biol. Sci. *273*, 2955–2963.
4. Deméré, T.A., and Berta, A. (2008). Skull anatomy of the Oligocene toothed mysticete *Aetioceus weltoni* (Mammalia; Cetacea): implications for mysticete evolution and functional anatomy. Zool. J. Linn. Soc. *154*, 308–352.
5. Fitzgerald, E.M.G. (2010). The morphology and systematics of *Mammalodon colliveri* (Cetacea: Mysticeti), a toothed mysticete from the Oligocene of Australia. Zool. J. Linn. Soc. *158*, 367–476.
6. Steeman, M.E. (2007). Cladistic analysis and a revised classification of fossil and recent mysticetes. Zool. J. Linn. Soc. *150*, 875–894.
7. Marx, F.G., Tsai, C.-H., and Fordyce, R.E. (2015). A new Early Oligocene toothed 'baleen' whale (Mysticeti: Aetiocetidae) from western North America: one of the oldest and the smallest. R. Soc. Open Sci. *2*, 150476.
8. Marx, F.G., Lambert, O., and Uhen, M.D. (2016). Cetacean Paleobiology (John Wiley and Sons).
9. Martini, E. (1971). Standard Tertiary and Quaternary calcareous nannoplankton zonation. Proceecings of the Second Planktonic Conference, Roma, 1970 *2*, 739–785.
10. Agnini, C., Fornaciari, E., Raffi, I., Catanzariti, R., Pälike, H., Backman, J., and Rio, D. (2014). Biozonation and biochronology of Paleogene calcareous nannofossils from low and middle latitudes. Newsl. Stratigr. *47*, 131–181.
11. Martínez-Cáceres, M., Lambert, O., and de Muizon, C. (2017). The anatomy and phylogenetic affinities of *Cynthiacetus peruvianus*, a large dorudontine basilosaurid (Cetacea, Mammalia) from the late Eocene of Peru. Geodiversitas *39*, 7–163.
12. Sanders, A.E., and Geisler, J.H. (2015). A new basal odontocete from the upper Rupelian of South Carolina, USA, with contributions to the systematics of *Xenorophus* and *Mirocetus* (Mammalia, Cetacea). J. Vertebr. Paleontol. *35*, e890107.
13. Uhen, M.D. (2004). Form, function, and anatomy of *Dorudon atrox* (Mammalia, Cetacea): an archaeocete from the middle to late Eocene of Egypt. Univ. Michigan Papers Paleontol. *34*, 1–222.
14. Geisler, J.H., McGowen, M.R., Yang, G., and Gatesy, J. (2011). A supermatrix analysis of genomic, morphological, and paleontological data from crown Cetacea. BMC Evol. Biol. *11*, 112.
15. Tsai, C.-H., and Ando, T. (2016). Niche partitioning in Oligocene toothed mysticetes (Mysticeti: Aetiocetidae). J. Mamm. Evol. *23*, 33–41.
16. Lambert, O., Bianucci, G., Post, K., de Muizon, C., Salas-Gismondi, R., Urbina, M., and Reumer, J. (2010). The giant bite of a new raptorial sperm whale from the Miocene epoch of Peru. Nature *466*, 105–108.
17. Pyenson, N.D., and Sponberg, S.N. (2011). Reconstructing body size in extinct crown Cetacea (Neoceti) using allometry, phylogenetic methods and tests from the fossil record. J. Mamm. Evol. *18*, 269–288.
18. Fitzgerald, E.M.G. (2012). Archaeocete-like jaws in a baleen whale. Biol. Lett. *8*, 94–96.
19. Marx, F.G., Hocking, D.P., Park, T., Ziegler, T., Evans, A.R., and Fitzgerald, E.M.G. (2016). Suction feeding preceded filtering in baleen whale evolution. Mem. Mus. Vic. *75*, 71–82.
20. Sanchez, J.A., and Berta, A. (2010). Comparative anatomy and evolution of the odontocete forelimb. Mar. Mamm. Sci. *26*, 140–160.
21. Werth, A.J. (2006). Mandibular and dental variation and the evolution of suction feeding in Odontoceti. J. Mammal. *87*, 579–588.
22. Johnston, C., and Berta, A. (2011). Comparative anatomy and evolutionary history of suction feeding in cetaceans. Mar. Mamm. Sci. *27*, 493–513.
23. Fahlke, J.M. (2012). Bite marks revisited–evidence for middle-to-late Eocene *Basilosaurus isis* predation on *Dorudon atrox* (both Cetacea, Basilosauridae). Palaeontol. Electronica *15*, 1–16.
24. Snively, E., Fahlke, J.M., and Welsh, R.C. (2015). Bone-breaking bite force of *Basilosaurus isis* (Mammalia, Cetacea) from the late Eocene of Egypt estimated by finite element analysis. PLoS ONE *10*, e0118380.
25. Berta, A., Lanzetti, A., Ekdale, E.G., and Deméré, T.A. (2016). From teeth to baleen and raptorial to bulk filter feeding in mysticete cetaceans: the role of paleontological, genetic, and geochemical data in feeding evolution and ecology. Integr. Comp. Biol. *56*, 1271–1284.
26. Hocking, D.P., Marx, F.G., Park, T., Fitzgerald, E.M.G., and Evans, A.R. (2017). A behavioural framework for the evolution of feeding in predatory aquatic mammals. Proc. Biol. Sci. *284*, 20162750.
27. Deméré, T.A., McGowen, M.R., Berta, A., and Gatesy, J. (2008). Morphological and molecular evidence for a stepwise evolutionary transition from teeth to baleen in mysticete whales. Syst. Biol. *57*, 15–37.
28. Ford, J.K.B., Ellis, G.M., Matkin, C.O., Wetklo, M.H., Barrett-Lennard, L.G., and Withler, R.E. (2011). Shark predation and tooth wear in a population of northeastern Pacific killer whales. Aquat. Biol. *11*, 213–224.
29. Lambert, O., de Muizon, C., and Bianucci, G. (2013). The most basal beaked whale *Ninoziphius platyrostris* Muizon, 1983: clues on the evolutionary history of the family Ziphiidae (Cetacea: Odontoceti). Zool. J. Linn. Soc. *167*, 569–598.
30. Benke, H. (1993). Investigations on the osteology and the functional morphology of the flipper of whales and dolphins (Cetacea). Investigations on Cetacea *24*, 9–252.
31. Thewissen, J.G., Cohn, M.J., Stevens, L.S., Bajpai, S., Heyning, J., and Horton, W.E., Jr. (2006). Developmental basis for hind-limb loss in dolphins and origin of the cetacean bodyplan. Proc. Natl. Acad. Sci. USA *103*, 8414–8418.
32. Fordyce, R.E. (2002). *Simocetus rayi* (Odontoceti: Simocetidae) (new species, new genus, new family), a bizarre new archaic Oligocene dolphin from the eastern North Pacific. Smith. Contr. Paleobiol. *93*, 185–222.
33. Uhen, M.D. (2008). A new *Xenorophus*-like odontocete cetacean from the Oligocene of North Carolina and a discussion of the basal odontocete radiation. J. Syst. Palaeontology *6*, 433–452.
34. Barnes, L.G., Goedert, J.L., and Furusawa, H. (2001). The earliest known echolocating toothed whales (Mammalia; Odontoceti): preliminary observations of fossils from Washington State. Mesa Southwest Mus. Bull. *8*, 91–100.
35. Swofford, D.L. (2001). PAUP*: phylogenetic analysis using parsimony (*and other methods), version 4b10 (Sinauer Associates).
36. Dunbar, R.B., Marty, R.C., and Baker, P.A. (1990). Cenozoic marine sedimentation in the Sechura and Pisco basins, Peru. Palaeogeogr. Palaeoclimatol. Palaeoecol. *77*, 235–261.
37. DeVries, T.J. (1998). Oligocene deposition and Cenozoic sequence boundaries in the Pisco Basin (Peru). J. S. Am. Earth Sci. *11*, 217–231.
38. DeVries, T.J., Navarez, Y., Sanfilippo, A., Malumian, N., and Tapia, P. (2006). New microfossil evidence for a late Eocene age of the Otuma Formation (Southern Peru). XIII Congreso Peruano de Geología, Lima, Peru, 615–618.

39. León, W., Aleman, A., Torres, V., Rosel, W., and De La Cruz, O. (2008). Estratigrafía, Sedimentología y Evolución Tectónica de la Cuenca Pisco Oriental (INGEMMET).

40. Steurbaut, E., and King, C. (1994). Integrated stratigraphy of the Mont-Panisel borehole section (151E340), Ypresian (Early Eocene) of the Mons Basin, SW Belgium. Bull. Soc. Belg. Géol. *102*, 175–202.

41. Steurbaut, E., and Sztrákos, K. (2008). Danian/Selandian boundary criteria and North Sea Basin-Tethys correlations based on calcareous nannofossil and foraminiferal trends in SW France. Mar. Micropaleontol. *67*, 1–29.

42. King, C., Underwood, C.J., and Steurbaut, E. (2014). Eocene stratigraphy of the Wadi Al-Hitan World Heritage Site and adjacent areas (Fayum, Egypt). Stratigraphy *11*, 185–234.

43. Perch-Nielsen, K. (1985). Cenozoic calcareous nannofossils. In Plankton Stratigraphy, H.M. Bolli, J.B. Saunders, and K. Perch-Nielsen, eds. (Cambridge University Press), pp. 427–554.

44. Fornaciari, E., Agnini, C., Catanzariti, R., Rio, D., Bolla, E.M., and Valvasoni, E. (2010). Mid-Latitude calcareous nannofossil biostratigraphy and biochronology across the middle to late Eocene transition. Stratigraphy *7*, 229–264.

STAR★METHODS

KEY RESOURCES TABLE

REAGENT or RESOURCE	SOURCE	IDENTIFIER
Deposited Data		
Character-taxon matrix	This paper; [1]	http://morphobank.org/permalink/?P2655
Software and Algorithms		
PAUP 4.0a150	[35]	http://paup.sc.fsu.edu/

CONTACT FOR REAGENT AND RESOURCE SHARING

Further information and requests for resources and reagents should be directed to and will be fulfilled by the Lead Contact, Olivier Lambert (olivier.lambert@naturalsciences.be).

METHOD DETAILS

Geological Context and Biostratigraphy

Geological context

The stratigraphy of the Cenozoic succession cropping out in the onland Pisco Basin of southern Peru has been described by Dunbar et al. [36] and DeVries [37]. The Paleogene units include, from oldest to youngest, the middle to upper Eocene Los Choros and Yumaque formations, and the uppermost Eocene to lower Oligocene Otuma Formation [38]. The Los Choros Formation is composed of nearshore and inner shelf, medium- to coarse-grained, massive and cross-laminated bioclastic sandstones with nodular horizons and, to a lesser extent, siltstone and mudstone [39]. The overlying Yumaque Formation comprises finely laminated or massive, green-gray phosphatic diatomaceous siltstones rich in fish scales; it represents deposition in distal, low-energy marine settings.

In the course of this study, a 150 m-thick detailed stratigraphic section was measured in a coastal outcrop adjacent to Media Luna Bay (Figure S1). The measured stratigraphy spans from the uppermost portion of the Los Choros Formation (14°36'15.2"S - 75°54'48.4"W) through the Yumaque Formation to the lowermost portion of the overlying Otuma Formation (14°36'3.6"S - 75°54'55.5"W). Several samples for biostratigraphic analysis were collected from the Yumaque Formation and the lower portion of the Otuma Formation and their relative stratigraphic position with respect to that of *Mystacodon selenensis* MUSM 1917 is shown in Figure S1.

Calcareous nannofossil biostratigraphy and geochronological implications

The calcareous nannofossil investigation is based on a thorough study of 37 samples, almost evenly spaced over the about 128 m thick Yumaque Formation and the lower 16 m of the overlying Otuma Formation. Samples (ML13-0 to ML13-4 and ML3 to ML34, collected in 2013 and 2015 respectively, Table S1) were processed following the preparation and investigation procedures explained by Steurbaut and King [40] and Steurbaut and Sztrákos [41]. The CNE (Calcareous Nannofossil Eocene) biozonation of Agnini et al. [10], the upper part of which (CNE10 to CNE21) is defined in the central western Atlantic ODP Sites 1051 and 1052 and the southeastern Atlantic DSDP Site 522, is applied here. Additional biohorizons used to subdivide the middle and upper Eocene interval in these Atlantic borehole sections [10] and in onshore sections of the Fayum, N Egypt [42], have also been recorded, allowing a high-resolution dating. Among these, are the lowest occurrences (LO) of *Chiasmolithus oamaruensis* and *Isthmolithus recurvus*, defining respectively the base of standard zones NP18 and NP19/20 of Martini [9]. The age estimates of the biohorizons are taken from Agnini et al. [10]. The taxonomy is essentially from Perch-Nielsen [43], taking into account the subsequent modifications by Fornaciari et al. [44] and Steurbaut in King et al. [42]. Rock samples and microscopic slides are stored at the Royal Belgian Institute of Natural Sciences (RBINS), Brussels, Belgium. The following abbreviations are used: LO = lowest occurrence, LCO = lowest common occurrence, HO = highest occurrence, HCO = highest common occurrence; Fm = Formation; Ma = million years ago.

Calcareous nannofossils are irregularly distributed in the Yumaque Fm, essentially because of episodic (primary and/or secondary) decalcification. Moderately rich, but generally poorly to moderately preserved assemblages are recorded in the lowermost 65 m. This strongly contrasts with the upper 60 m, which is devoid of nannofossils, except for two levels in the uppermost 15 m, which contain poorly preserved, impoverished assemblages (Table S1). The biostratigraphic and biochronological interpretations presented here are based on the identification of the following nannofossil events: 1. the LO (1 specimen) of *Cribrocentrum reticulatum* between ML3 and ML13-0, dated around 42.6 Ma; 2. the LO of *Dictyococcites bisectus* between ML10 and ML11, dated at 40.34 Ma; 3. the HCO of *Sphenolithus spiniger* between ML11 and ML12, dated around 40.1 Ma; 4. the HO of *Sphenolithus obtusus* between ML13 and ML14, dated at 38.47 Ma; 5. the LO of *Chiasmolithus oamaruensis* between ML14 and ML15, dated around 37.92 Ma (the LO of *C. oamaruensis* slightly predates the LCO of *Dictyococcites erbae*, according to data from Site ODP 10527 and the Fayum [42]); 6. the LO of *Isthmolithus recurvus* between ML16 and ML13-1, dated around 37.35 Ma (because of the co-occurrence of

I. recurvus and *C. oamaruensis,* and the absence of *Dictyococcites erbae*); 7. the LO of *Discoaster saipanensis* between ML13-2 and ML30, dated at 34.44 Ma.

The Yumaque Fm is bracketed between the LO of *Cribrocentrum reticulatum* below (1 specimen recorded at 2 m above its base; lower 2 m with badly preserved nannofossil assemblages) and the HO of *Discoaster saipanensis* above (present at 6 m below its top, but absent at 5 m above its top, and no nannofossil records in between). Accordingly it would range from the upper part of zone CNE13 to the lower part of zone CNE21 of Agnini et al. [10], or equally possibly, terminating in the underlying zone CNE20. Hence, the lower boundary of the Yumaque Fm should lie at approximately 42.7 Ma and its upper boundary at 34.4 Ma. Apparently it took about 8.3 myr to deposit this ca 127.65 m thick formation, which implies a mean sedimentation rate of 1.5 cm/kyr. Sedimentation rates are not constant throughout the Yumaque Fm, as shown by the estimated nannofossil-based ages recorded within the formation. Indeed, sedimentation rates seem to be progressively increasing during deposition from 1.2 cm/kyr in the lowermost 28 m, through 1.7 cm/kyr in the interval from 37 m to 46.5 m, to 2.3 cm/kyr in the uppermost 80 m of the Yumaque Fm.

The skeletal remains of *Mystacodon selenensis* MUSM 1917 were unearthed at 77.35 m above the base of the Yumaque Fm, which accumulated at a mean sedimentation rate of 1.5 cm/kyr. Using these parameters it is estimated that the time of burial of this early mysticete specimen postdates the onset of the Yumaque Fm by about 5.2 myr, and consequently occurred about 37.5 Ma. However, this date is not realistic and much too old, considering the fossil's position at 15 m (at least) above the LO of *Isthmolithus recurvus,* the age of which is estimated at about 37.35 Ma (Table S1). Its position within the upper middle part of the Yumaque Fm would be in favor for applying a much higher sedimentation rate, intermediate between 1.7 cm/kyr and 2.3 cm/kyr, calculated for the lower middle and upper parts of the Yumaque Fm, respectively. Increasing the sedimentation rate to a realistic value of 2 cm/kyr would imply that *M. selenensis* MUSM 1917 fossilized during the early late Eocene, at approximately 36.4 Ma (30 m above or 1.5 myr after the LO of *C. oamaruensis*, dated at 37.92 Ma), a conclusion that is entirely corroborated by the biostratigraphic and biochronological results.

Phylogenetic Analysis

The starting point of our parsimony analysis is the data matrix of Marx and Fordyce [1]. Because our analysis is mainly focused on the early radiations of mysticetes we retained only 24 taxa (out of 53) of Chaeomysticeti (baleen-bearing whales) of their matrix, representing most of the major clades of this group. The New Zealand undescribed taxa to which we did not have access during this study were excluded, but we retained the undescribed toothed mysticete from the Oligocene of North Carolina (ChM PV 4745) and added a new specimen (ChM PV 5720). Concerning the outgroup, we replaced *Zygorhiza kochii* with *Cynthiacetus peruvianus*, for which we had the holotype at hand, an almost complete skeleton with a perfectly preserved skull [11], and we replaced the odontocete *Waipatia maerewhenua* with the geologically older *Simocetus rayi*. With these changes, our analysis includes 38 taxa (4 outgroup and 34 ingroup) and the character list is that of Marx and Fordyce [1] with 272 characters (13 dental, 202 cranial, 23 mandibular, 27 postcranial, and 7 soft anatomy), among which 25 multistate characters are treated as additive (see Data S1). The heuristic search with equally weighted characters was performed using PAUP 4.0a150 [35]; it resulted in two equally parsimonious trees, in which the Mysticeti were monophyletic and MUSM 1917 was the earliest branching member of the suborder. Bremer support values were calculated (Figure 4), with an average value of 5.6 for the 32 ingroup nodes.

QUANTIFICATION AND STATISTICAL ANALYSIS

Two equations were used for estimating the total body length (TL) of MUSM 1917, both based on the bizygomatic width of the skull (Table S2):

(1) Equation of Pyenson and Sponberg [17] for stem mysticetes:

$$\log(\mathrm{TL}) = 0.92 * (\log(\mathrm{BIZYG}) - 1.72) + 2.68$$

(2) Equation of Lambert et al. [16] for extant and extinct mysticetes:

$$\mathrm{TL} = 8.209 * \mathrm{BIZYG} + 66.69$$

DATA AND SOFTWARE AVAILABILITY

The character-taxon matrix reported in this paper is available in MorphoBank under the project number 2655 (http://morphobank.org/permalink/?P2655).